

Article

Mixed-Potential Gas Sensors Using an Electrolyte Consisting of Zinc Phosphate Glass and Benzimidazole

Takafumi Akamatsu *, Toshio Itoh and Woosuck Shin

National Institute of Advanced Industrial Science and Technology (AIST),
Inorganic Functional Materials Research Institute, 2266-98, Anagahora, Shimo-Shidami,
Moriyama-ku, Nagoya-shi 463-8560, Japan; itoh-toshio@aist.go.jp (T.I.); w.shin@aist.go.jp (W.S.)

* Correspondence: t-akamatsu@aist.go.jp; Tel.: +81-52-736-7602

Academic Editor: W. Rudolf Seitz

Received: 16 November 2016; Accepted: 3 January 2017; Published: 5 January 2017

Abstract: Mixed-potential gas sensors with a proton conductor consisting of zinc metaphosphate glass and benzimidazole were fabricated for the detection of hydrogen produced by intestinal bacteria in dry and humid air. The gas sensor consisting of an alumina substrate with platinum and gold electrodes showed good response to different hydrogen concentrations from 250 parts per million (ppm) to 25,000 ppm in dry and humid air at 100–130 °C. The sensor response varied linearly with the hydrogen and carbon monoxide concentrations due to mass transport limitations. The sensor responses to hydrogen gas (e.g., -0.613 mV to 1000 ppm H₂) was higher than those to carbon monoxide gas (e.g., -0.128 mV to 1000 ppm CO) at 120 °C under atmosphere with the same level of humidity as expired air.

Keywords: gas sensor; mixed-potential; zinc phosphate glass; hydrogen

1. Introduction

Expired air contains over 100 different gases in a humid atmosphere at low concentrations, ranging from sub parts per billion (ppb) to parts per million (ppm), including hydrogen (H₂), carbon monoxide (CO), and various volatile organic compounds (VOCs) [1–6]. Expired air can provide information that is useful for monitoring human health. The concentration of H₂ in expired air has been used to monitor microbial metabolism in the colon [1–4], since H₂ is produced by intestinal bacteria. High-performance gas sensors provide a simple and non-invasive method to monitor expired air, and are therefore one of the most promising approaches for the early detection of diseases.

Mixed-potential gas sensors using yttria-stabilized zirconia (YSZ) electrolyte have been investigated for the detection of H₂, CO, nitric oxide, ethanol, and methane [7–11]. These gas sensors must be operated at temperatures above 500 °C to provide both satisfactory response rates against target gases and good gas selectivity. These gas sensors require a heater to maintain the operating temperature above 500 °C, which results in high power consumption. Mixed-potential gas sensors that use electrolytes with high proton conductivity—such as Nafion, zirconium phosphate, and antimonic acid—have been reported to function at reduced operating temperatures [12–15]. However, these electrolytes must be impregnated with water to achieve high proton conductivity, which necessitates the inclusion of a complicated humidity control system to allow these sensors to operate at room temperature and under high humidity. Moreover, these gas sensors show low selectivity for H₂ against CO. One approach to overcoming this challenge is to use anhydrous proton conductors at an intermediate temperature between 100 and 300 °C. However, to the best

of our knowledge, no mixed-potential gas sensors using a high-proton-conductivity electrolyte at intermediate temperatures have been reported (Table 1).

Oine et al. and Kato et al. have successfully prepared an anhydrous electrolyte that demonstrates high proton conductivity at temperatures between 100 and 200 °C by the reaction of zinc metaphosphate glass with benzimidazole [16,17]. This material has been investigated as an electrolyte in electrochemical devices that operate at intermediate temperatures, such as fuel cells. Thus, we suggest that this anhydrous electrolyte has the potential to be applied as a mixed-potential gas sensor.

In this study, we prepared a mixed-potential gas sensor using an electrolyte consisting of zinc metaphosphate glass and benzimidazole, and the sensor's response to H₂ gas in both humid and dry air was investigated. An initial investigation of the sensor's response to CO in humid air was also conducted to determine its selectivity for H₂ against other gases.

Table 1. Typical examples of mixed-potential gas sensors for H₂ detection. YSZ: yttria-stabilized zirconia.

Sensor Materials	Sensor Structure		Sensing Temperature	H ₂ Concentration	References
	Sensing Electrode	Reference Electrode			
YSZ	ZnO	Pt	400–600 °C	50–500 ppm	[7]
Sb ₂ O ₅ ·4H ₂ O	Pt	Au	Room temperature	200–10,000 ppm	[12]
Zr(HPO ₄) ₂ ·nH ₂ O	Pt	Ag	Room temperature	300–10,000 ppm	[14]
Sn _{0.9} In _{0.1} P ₂ O ₇	Pt/C	Pt	30 °C	100–30,000 ppm	[15]

2. Materials and Methods

A glass with a nominal molar ratio of 1:1 ZnO:P₂O₅ was prepared by melting a batch mixture of the commercially available reagent-grade chemicals ZnO and H₃PO₄ in a platinum crucible at 1100 °C in air for 30 min. The melt was poured onto an iron plate and quenched by iron pressing to make glass flakes. The glass flakes were milled using an alumina mortar and pestle to below 100 μm in diameter. The glass powder was mixed with benzimidazole, and the mixture was heated at 170 °C for 12 h to make an electrolyte. The weight ratio of the glass powder and benzimidazole was 1:3. Details of the procedures and electrolyte properties have been previously reported [17].

The sensor element we constructed is shown schematically and as a photograph in Figure 1. The electrolyte was deposited on an alumina substrate with platinum (Pt) and gold (Au) electrodes, with both the electrode gap and electrode width being 1 mm. Finally, the electrolyte-coated substrate was heated from behind by placing the assembly on a hotplate, resulting in the formation of an electrolyte membrane on the substrate.

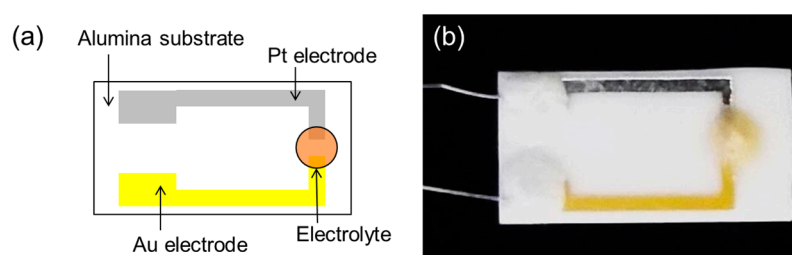


Figure 1. The structure of the sensor: (a) schematic illustration; and (b) optical image.

The sensor element was placed in a test chamber and heated to 80–130 °C in an electrical tube furnace. Synthetic dry air was introduced into the chamber for 20 min, and a gas mixture of H₂ or CO in synthetic dry air was then injected for 20 min. The gas mixture flow rate was 200 mL/min. Synthetic dry air and H₂ or CO in synthetic air were prepared by mixing 99.99% N₂ gas, N₂-balanced 5% H₂ gas, N₂-balanced 5% CO gas, and 99.5% O₂ gas. The O₂ content of synthetic dry air and that of H₂ or CO in synthetic dry air were both 20 vol %. The H₂ or CO gas concentrations in synthetic dry air were

controlled at values of 250, 500, 1000, 2500, 5000, 10,000, and 25,000 ppm. Synthetic humid air was prepared by passing air through ion-exchanged water at 25 °C before flowing to a test chamber.

The potential difference (electromotive force, EMF) between Pt and Au electrodes of the sensor element was recorded using a data logger (midi Logger GL220; Graphtec Corp., Yokohama, Japan). During the potential difference measurements, the Pt electrode was always connected to the positive terminal of the data logger. The EMFs of the sensor element in the air and gas mixtures are denoted as V_a and V_g , respectively. The sensor response (ΔV) is defined as $\Delta V = V_a - V_g$.

3. Results and Discussion

Figure 2 shows that upon exposure to 25,000 ppm H_2 in humid and dry air at 80 °C, 100 °C, 120 °C, and 130 °C, the sensor's response increased with increasing operating temperature. Miura et al. described the potential response upon exposure to hydrogen in humid gas of a solid-state sensor that used a proton-conductor [12]. The EMF depends on the electrochemical oxidation and reduction reactions occurring at the Pt and Au electrodes:



A mixed potential is established when the electron transfer rates of the hydrogen oxidation and the oxygen reduction are same. Since the kinetics of the sensor's Pt and Au electrodes are different from those of the oxidation of H_2 to water, the mixed-potential generated at each electrode varies, and thus ΔV varies in accordance with the H_2 gas concentration. We reported that the sensor response to H_2 in synthetic dry air at 150 °C is higher than that at 130 °C [18]. However, in this paper, when the sensor response to H_2 was investigated at 140 °C, the EMF was unstable and gradually decreased over the measuring time, and the sensor showed no response to H_2 gas (not pictured). This behavior may result from changes in the electrochemical properties of the electrolyte due to volatilization of the benzimidazole in the electrolyte, because the flash point of benzimidazole was 143 °C [19]. Therefore, the optimum operating temperature of the sensor is below 140 °C. In general, the sensor responses are similar at each temperature. At 120 °C, the sensor response in dry air is higher, whereas for the other temperatures, the sensor response in humid air is higher. The electrolyte derived from zinc metaphosphate glass and benzimidazole is an anhydrous proton-conducting material, and has good water durability [16,17]. Therefore, the electrical properties of the electrolyte were not changed by water vapor, and the sensor responses using the electrolyte was considered to be seen even in humid air. However, the difference between the sensor responses to H_2 in dry air and humid air was significant. In future study, we will investigate the cycle characteristics and error evaluation of the sensor response.

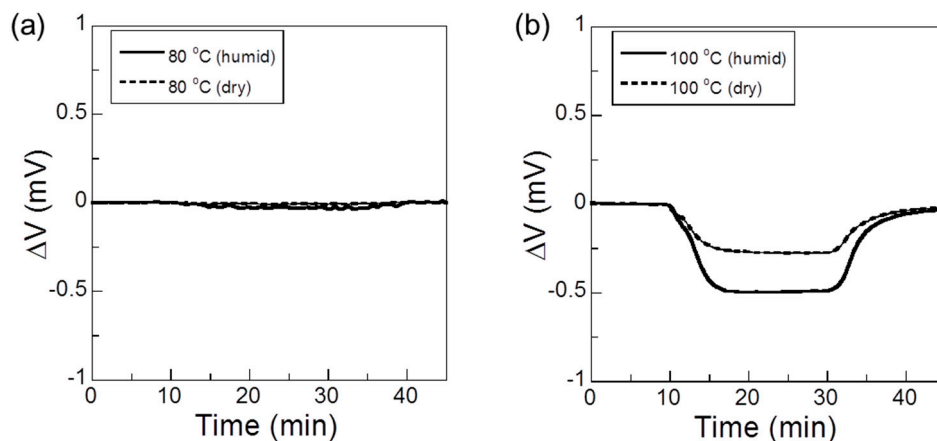


Figure 2. Cont.

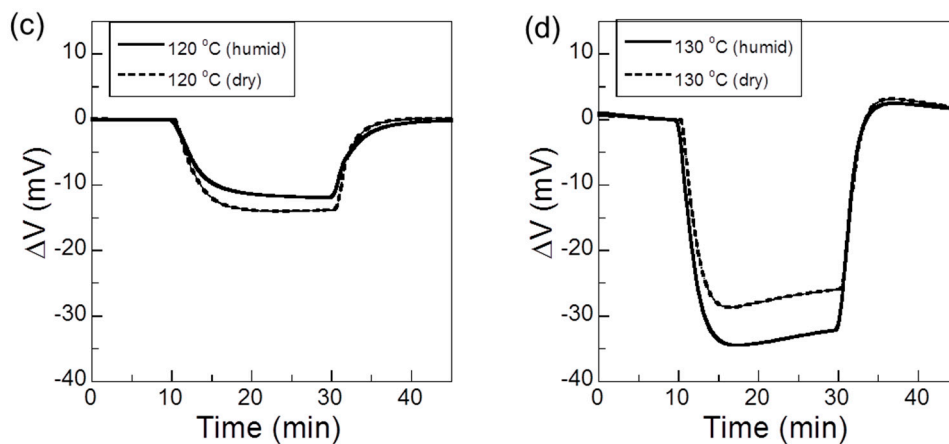


Figure 2. Sensor responses to 25,000 ppm H_2 in humid and dry air at (a) 80 °C; (b) 100 °C; (c) 120 °C; and (d) 130 °C.

Figure 3 shows the sensor responses to H_2 concentrations ranging from 250 ppm to 25,000 ppm in humid air at 120 °C. These results show that the ΔV of the sensor began to decrease rapidly on exposure to H_2 , and the response was stronger for higher concentrations of H_2 . Figure 2 shows that the difference between the sensor responses to H_2 in dry air and humid air was large at this stage. In order to detect H_2 with high accuracy, error evaluation of the sensor response under different humidity conditions must be investigated. The model designed by Miura et al. suggests that a linear relationship exists between the logarithm of the H_2 concentration and ΔV , assuming a Tafel-like equation for the polarization behavior of the oxidation and reduction reactions at the electrode [12]. The ΔV can thus be expressed in the form:

$$\Delta V = a + b \log C_{H_2} \quad (3)$$

where a and b are constants, and C_{H_2} is the concentration of H_2 . Figure 4 shows the relationship between the sensor response and the logarithm of the H_2 concentration. The least squares regression analysis of the sensor can be expressed as follows:

$$\Delta V = 13.1 - 4.7 \log C_{H_2}, R = 0.819 \quad (4)$$

where the C_{H_2} is the concentration of H_2 , and R is the correlation coefficient. The sensitivity of the sensor was -4.7 mV/decade. However, no good linear relationship between the logarithm of H_2 concentration and ΔV of the sensor was obviously found.

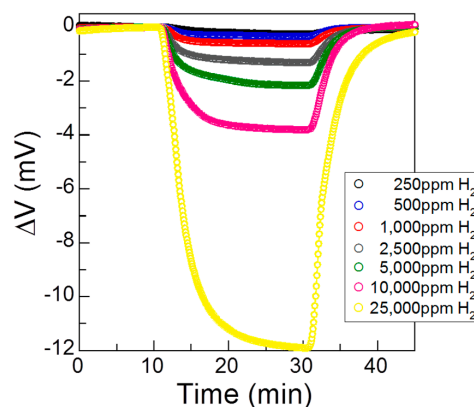


Figure 3. Sensor response to different concentrations of H_2 in humid air at 120 °C.

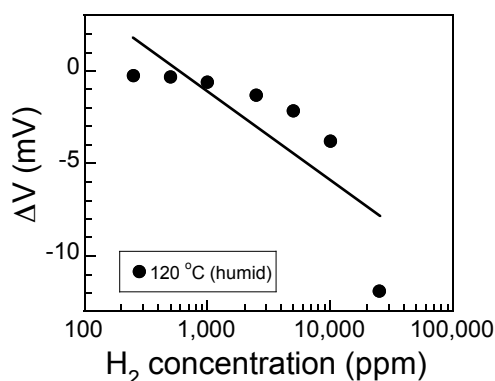


Figure 4. The relationship between sensor response and the log of the H₂ concentration in humid air at 120 °C. The solid line shows the least-squares linear fit.

According to Garzon et al., if the concentration of the sensed gas (H₂) is much lower than the concentration of O₂, a linear relationship between the H₂ concentration and ΔV exists because of the diffusional mass transport limitation [8]. In this case, ΔV can be expressed as

$$\Delta V = a + K C_{H_2} \quad (5)$$

where a and K are constants. Figure 5 shows the relationship between sensor response and the H₂ concentration. The sensor response was adequately linear. The least squares regression analysis of the sensor can be expressed as follows:

$$\Delta V = 0.021 - 0.00046 C_{H_2}, R = 0.996 \quad (6)$$

where C_{H_2} is the concentration of H₂, and R is the correlation coefficient. The sensitivity of the sensor was -0.00046 mV/ppm. R for Equation (6) was higher than that for Equation (4). This suggested that the oxidation reaction of H₂ may be mass transport-limited.

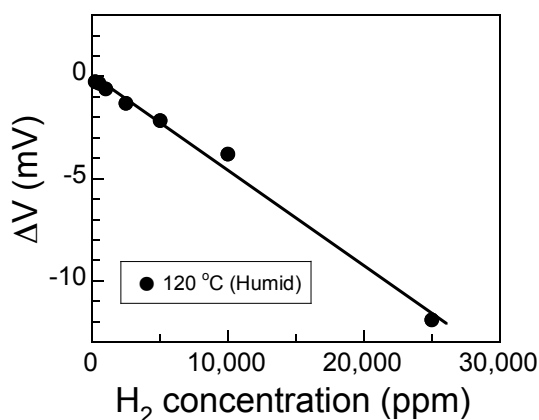


Figure 5. The relationship between the sensor response and the H₂ concentration in humid air at 120 °C. The solid line shows the least-squares linear fit.

Figure 6 shows the sensor's responses to CO in humid air at 120 °C and at concentrations ranging from 250 to 25,000 ppm. When the sensor was exposed to these conditions, its ΔV decreased rapidly, and the response decreased as the CO concentration increased. In CO gas sensing, the oxidation reaction of CO can take place simultaneously at both the Pt and Au electrodes:



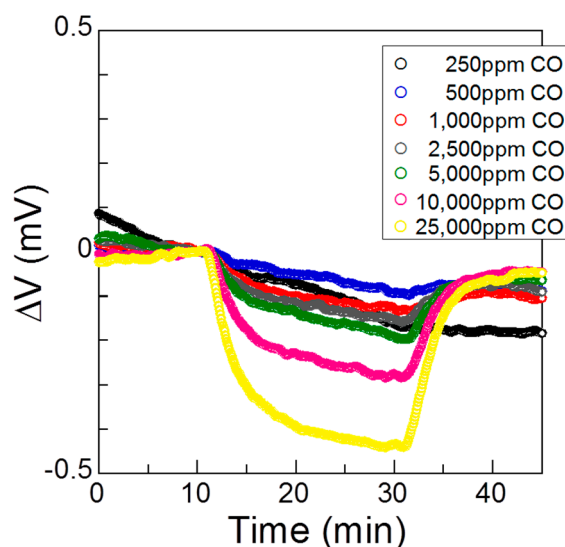


Figure 6. Sensor responses to different concentrations of CO in humid air at 120 °C.

Figure 7 shows the relationship between the sensor response and the logarithm of the CO concentration, and the relationship between the sensor response and the CO concentration in humid air at 120 °C. The equations of the relationship between the sensor response and CO concentration were determined from Equations (3) and (5), respectively:

$$\Delta V = 0.376 - 0.168 \log C_{CO}, R = 0.939 \quad (8)$$

$$\Delta V = 0.101 - 1.015 \times 10^{-6} C_{CO}, R = 0.977 \quad (9)$$

where C_{CO} is the concentration of CO and R is the correlation coefficient. Since R is slightly larger for Equation (9) than for Equation (8), the oxidation reaction of CO may be mass-transport-limited, as seen for the H_2 gas sensing.

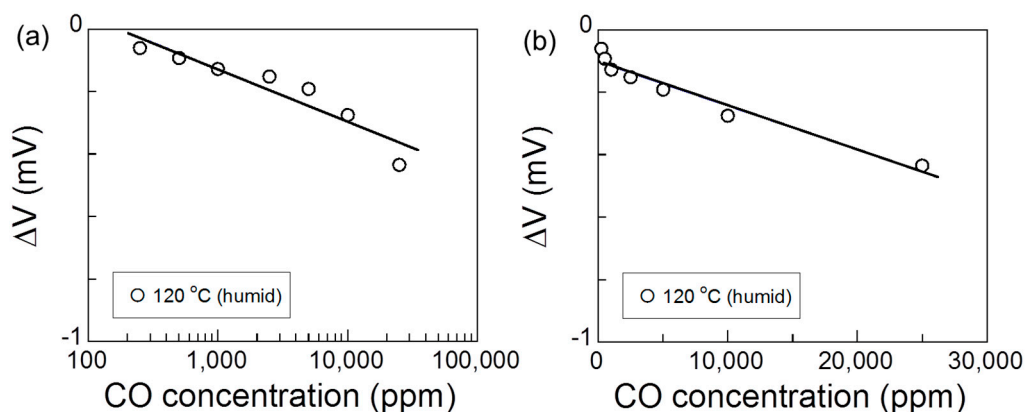


Figure 7. (a) The relationship between the sensor response and the logarithm of the CO concentration and (b) the relationship between the sensor response and the CO concentration in humid air at 120 °C. The solid lines show the least-squares linear fit.

The sensor responses to 1000 ppm H_2 and 1000 ppm CO were determined to be -0.613 mV and -0.128 mV, respectively, in humid air at 120 °C. These responses are lower than those seen for mixed-potential gas sensors that used proton conductor operating at around room temperature (-190 mV for 1000 ppm H_2 and -120 mV for 1000 ppm CO) [12]. The value of H_2 selectivity against

CO ($S_{H_2/CO}$) was determined using the equation $S_{H_2/CO} = \Delta V_{H_2} / \Delta V_{CO}$, where ΔV_{H_2} is the sensor's response at 1000 ppm H₂, and ΔV_{CO} is the sensor response at 1000 ppm CO. The $S_{H_2/CO}$ of our sensor was 4.8, and that of the sensor using a proton conductor operating at around room temperature was 1.6 [12].

Semiconductor gas sensors using n-type SnO₂ have been investigated for several decades for their high response to inflammable gases, such as H₂, CO, CH₄, and C₂H₅OH [20,21]. However, their low selectivity for H₂ over CO was regarded as a problem to be solved. Moon et al. focused on the use of a CuO-doped SnO₂-ZnO composite material to improve the gas selectivity, and reported a selectivity of ~4 for H₂ (200 ppm) over CO (200 ppm) at 350 °C [21]. The sensor reported herein—which used an electrolyte consisting of zinc metaphosphate glass and benzimidazole—showed a higher selectivity for H₂ against CO than the sensor reported by Moon et al. However, our sensor's response to H₂ is currently inferior, thus optimization of the sensor design is required to achieve a greater response. Further investigations of the sensor's response to other interfering species (such as CH₄ and VOCs) will be conducted in the future.

4. Conclusions

In this study, we have investigated the responses of a mixed-potential gas sensor that used a proton conductor composed of zinc metaphosphate glass and benzimidazole for the detection of H₂ (produced by intestinal bacteria) and CO gas (an interference in expired air). The gas sensor showed good sensor response to H₂ in the concentration range 250–25,000 ppm under atmosphere having the same level of humidity as expired air at 120 °C. The mixed-potential gas sensor without a heater can detect gases under the atmosphere at temperatures in the range 100–130 °C. The sensor response varied linearly with the hydrogen and carbon monoxide concentrations, as expected under mass-transport-limited conditions. The gas sensor showed high gas selectivity for H₂ against CO ($S_{H_2/CO} = 4.8$).

Acknowledgments: This work was supported in part by Naito Research Grant.

Author Contributions: T.A. performed the experiments and prepared the manuscript. T.I. and W.S. helped in designing the experiments and provided valuable guidance. All authors discussed the results of the manuscript.

Conflicts of Interest: The authors declare no conflict of interest.

References

1. Simouchi, A.; Nose, K.; Yamaguchi, M.; Ishiguro, H.; Kondo, T. Breath hydrogen produced by ingestion of commercial hydrogen enriched water and milk. *Biomark. Insights* **2009**, *4*, 27–33.
2. Behall, K.M.; Scholfield, D.J.; van der Sluijs, A.M.; Hallfrisch, J. Breath hydrogen and methane expiration in men and women after oat extract consumption. *J. Nutr.* **1998**, *128*, 79–84. [[PubMed](#)]
3. Shin, W.; Nishibori, M.; Izu, N.; Itoh, T.; Matsubara, I.; Nose, K.; Shimouchi, A. Monitoring breath hydrogen using thermoelectric sensor. *Sens. Lett.* **2011**, *9*, 684–687. [[CrossRef](#)]
4. Shin, W. Medical applications of breath hydrogen measurements. *Anal. Bioanal. Chem.* **2014**, *406*, 3931–3939. [[CrossRef](#)] [[PubMed](#)]
5. Roberge, M.T.; Finley, J.W.; Lukaski, H.C.; Borberding, A.J. Evaluation of the pulsed discharge helium ionization detector for the analysis of hydrogen and methane in breath. *J. Chromatogr. A* **2004**, *1027*, 19–23. [[CrossRef](#)] [[PubMed](#)]
6. Risby, T.H.; Amann, A.; Smith, D. *Breath Analysis for Clinical Diagnostics and Therapeutic Monitoring*; World Scientific: London, UK, 2005; pp. 251–267.
7. Lu, G.; Miura, N.; Yamazoe, N. High-temperature hydrogen sensor based on stabilized zirconia and a metal oxide electrode. *Sens. Actuators B Chem.* **1996**, *35–36*, 130–135. [[CrossRef](#)]
8. Garzon, F.H.; Mukundan, R.; Brosha, E.L. Solid-state mixed potential gas sensors: Theory, experiments and challenges. *Solid State Ionics* **2000**, *136–137*, 633–638. [[CrossRef](#)]

9. Park, J.; Yoon, B.Y.; Park, C.O.; Lee, W.-J.; Lee, C.B. Sensing behavior and mechanism of mixed potential NO_x sensors using NiO, NiO(+YSZ) and CuO oxide electrodes. *Sens. Actuators B Chem.* **2009**, *135*, 516–523. [[CrossRef](#)]
10. Liu, F.; Yang, X.; Yu, Z.; Wang, B.; Guan, Y.; Liang, X.; Sun, P.; Liu, F.; Gao, Y.; Lu, G. Highly sensitive mixed-potential type ethanol sensors based on stabilized zirconia and ZnNb₂O₆ sensing electrode. *RSC Adv.* **2016**, *6*, 27197–27204. [[CrossRef](#)]
11. Tho, N.D.; Huong, D.V.; Ngan, P.Q.; Thai, G.H.; Thu, D.T.A.; Thu, D.T.; Tuoi, N.T.M.; Toan, N.N.; Giang, H.T. Effect of sintering temperature of mixed potential sensor Pt/YSZ/LaFeO₃ on gas sensing performance. *Sens. Actuators B Chem.* **2016**, *224*, 747–754. [[CrossRef](#)]
12. Miura, N.; Harada, T.; Shimizu, Y.; Yamazoe, N. Cordless solid-state hydrogen sensor using proton-conductor thick film. *Sens. Actuators B Chem.* **1990**, *1*, 125–129. [[CrossRef](#)]
13. Miura, N.; Kato, H.; Yamazoe, N.; Seiyama, T. A proton conductor gas sensor operative at ordinary temperature. *Denki Kagaku* **1982**, *50*, 858–859.
14. Miura, N.; Kato, H.; Yamazoe, N.; Seiyama, T. An improved type of proton conductor sensor sensitive to H₂ and CO at room temperature. *Chem. Lett.* **1983**, *12*, 1573–1576. [[CrossRef](#)]
15. Tomita, A.; Hibino, T.; Suzuki, M.; Sano, M. Proton conduction at the surface of Y-doped BaCeO₃ and its application to an air/fuel sensor. *J. Mater. Sci.* **2004**, *39*, 2493–2497. [[CrossRef](#)]
16. Oine, T.; Maeda, H.; Tsuzuki, T.; Nakayama, M.; Kasuga, T. Relationship between electrical conductivities and structure of hybrid materials derived from mixtures of zinc phosphate glasses with different phosphate-chain lengths and benzimidazole. *J. Solid State Electrochem.* **2015**, *19*, 907–912. [[CrossRef](#)]
17. Kato, H.; Kasuga, T. Preparation of proton-conducting hybrid materials by reacting zinc phosphate glass with benzimidazole. *Mater. Lett.* **2012**, *79*, 109–111. [[CrossRef](#)]
18. Akamatsu, T.; Itoh, T.; Shin, W. Mixed-potential gas sensors based on a noble electrolyte consisting of zinc metaphosphate glass and benzimidazole. In Proceedings of the IMCS 2016, Jeju Island, Korea, 10–14 July 2016.
19. Kumar, D.; Sharma, K. Benzimidazole, a versatile analogue. *Int. J. Pharm. Prof. Res.* **2012**, *3*, 555–560.
20. Yamazoe, N.; Kurokawa, Y.; Seiyama, T. Effects of additives on semiconductor gas sensors. *Sens. Actuators* **1983**, *4*, 283–289. [[CrossRef](#)]
21. Moon, W.J.; Yu, J.H.; Choi, G.M. The CO and H₂ gas selectivity of CuO-doped SnO₂-ZnO composite gas sensor. *Sens. Actuators B Chem.* **2002**, *87*, 464–470. [[CrossRef](#)]



© 2017 by the authors; licensee MDPI, Basel, Switzerland. This article is an open access article distributed under the terms and conditions of the Creative Commons Attribution (CC-BY) license (<http://creativecommons.org/licenses/by/4.0/>).